ICASSP 2024 - 2024 IEEE International Conference on Acoustics, Speech and Signal Processing (ICASSP) | 979-8-3503-4485-1/24/$31.00 ©2024 IEEE | DOI: 10.1109/ICASSP48485.2024.10447003

FREQUENCY ESTIMATION VIA SUB-NYQUIST UNLIMITED SAMPLING

Yuliang Zhu, Ruiming Guo, Peiyu Zhang and Ayush Bhandari

Dept. of Electrical and Electronic Engg., Imperial College London, SW7 2AZ, UK.
Email: {yuliang.zhu19,ruiming.guo,peiyu.zhang21,a.bhandari}@imperial.ac.uk

ABSTRACT

The problem of frequency estimation from sub-Nyquist samples has numerous applications across various disciplines and has been extensively studied in signal processing literature. Despite the existence of several algorithmic approaches, the full potential of these methods has not been realized due to the limitations of analog-to-digital converters (ADCs). In particular, accurately estimating frequency for high-dynamic-range signals that may saturate the ADC is still an interesting problem, regardless of the sub-Nyquist aspect. On a different note, the Unlimited Sensing Framework (USF) focuses on recovering large signals from folded samples but requires oversampling. In this paper, we propose a hardware-software co-design approach that allows for frequency estimation from folded samples at sub-Nyquist rates. Our key insight is that temporal redundancy can be eliminated by introducing channel redundancy. Surprisingly, our recovery guarantees are independent of the sampling rate. To achieve this, we introduce a novel multi-channel sampling pipeline coupled with a reconstruction algorithm. Beyond numerical experiments, we build customized hardware and validate our approach through lab experiments. This demonstrates the capabilities of our method in real-world scenarios while opening up new questions for the field.

***Index Terms*—** Sub-Nyquist sampling, frequency estimation, unlimited sampling, non-linear reconstruction.

1. INTRODUCTION

Digitization and Nyquist-Rate. Digital acquisition is the cornerstone of almost all modern technologies and applications. Underpinning the digital acquisition paradigm is the Shannon-Nyquist framework. This fundamental theorem sets a lower bound on the sampling rate for recovery of bandlimited inputs. Namely, recovery is possible provided that the sampling frequency is at least twice the bandwidth of the input—the Nyquist rate. This constitutes the conventional digital acquisition protocol for which its practical implementation utilizes analog-to-digital converters (ADCs).

Frequency Estimation at Sub-Nyquist Rate. Since the sampling rate and the bit-budget dictate the implementation costs of the ADCs, a natural question is: Can we achieve signal recovery at the sub-Nyquist sampling rate? The utility of this question has been long realized in the signal processing community and has motivated the sub-field of the so-called *sub-Nyquist sampling* [1–7]. Among many directions in sub-Nyquist sampling theory, one active topic is the frequency estimation of sinusoidal signals. As a fundamental problem in signal processing, frequency estimation has wide applications in many fields, spanning from radar, sonar, digital communications, to time-of-flight imaging [8]. However, in several scenarios, the sinusoidal signal to be estimated has intrinsically high bandwidth and the conventional Nyquist sampling becomes infeasible due to high power consumption and large cost.

This work is supported by the UK Research and Innovation council's FLF Program "Sensing Beyond Barriers" (MRC Fellowship award no. MR/S034897/1). Further details on Unlimited Sensing and upcoming materials on *reproducible research* are available via https://bit.ly/USF-Link.

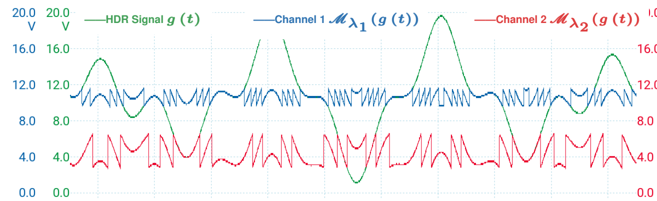

Fig. 1: Output of our multi-channel unlimited sampling architecture.

Related Work. Existing approaches on sub-Nyquist frequency estimation or sNyq-Ψ [1] can be categorized into two groups:

1) Stochastic Approaches. These approaches, in part pioneered by Vaidyanathan, Pal and co-workers, are based on multiple groups of sub-Nyquist samplers with co-prime sampling periods (see [7, 9]). The frequency aliasing caused by sub-Nyquist sampling is eliminated by the autocorrelation sequence estimated via the co-prime sampling period setups.
2) Deterministic Approaches. Based on the Chinese remainder theorem, these approaches have been studied to retrieve frequencies from multiple sub-Nyquist samples since the mid-90s. Much of the work has been spearheaded by Xia & co-workers [1–5]. By first retrieving aliased frequencies via standard spectral estimation techniques, these approaches remove ambiguity or frequency folding, via the Chinese remainder theorem.

From an algorithmic standpoint, sNyq-Ψ entails "unfolding" of tones that fold back or "alias" in the Fourier domain. Note that here aliasing takes place along the *abscissa*.

Frequency (Abscissa) versus Amplitude (Ordinate) Unfolding. In a different incarnation, this unfolding problem is also at the heart of the Unlimited Sensing Framework (USF) [10–13]. The difference being, in the USF, folding is purposefully injected to achieve folding of amplitude or ordinate, to prevent information loss via ADC clipping or saturation. Increasing the dynamic range of ADCs may avoid this issue, but would result in poor digital resolution due to quantization. This yields a fundamental trade-off between dynamic range and digital resolution in the Shannon-Nyquist Framework but is not a limitation in the USF [14, 15].

In the USF, before capturing pointwise samples, a modulo nonlinearity of the form

$$\mathscr{M}_\lambda : g \mapsto 2\lambda\left(\left[\!\left[\frac{g}{2\lambda}+\frac{1}{2}\right]\!\right]-\frac{1}{2}\right), \quad [\![g]\!] \stackrel{\text{def}}{=} g - \lfloor g \rfloor \qquad (1)$$

[1] We use sNyq-Ψ for *sub-Nyquist Frequency Estimation* as Ψ symbolizes a tuning-fork creating pure harmonics.

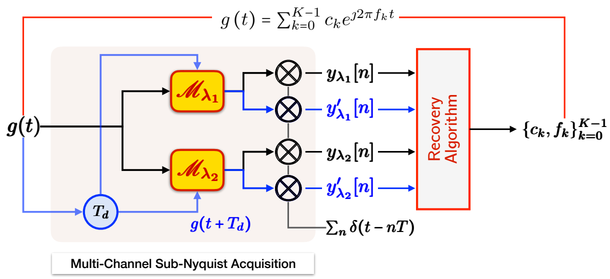

Fig. 2: The block diagram of the designed acquisition pipeline for sub-Nyquist Unlimited Sampling (sNyqλ-Ψ).

where $\lfloor g \rfloor = \sup \{ k \in \mathbb{Z} | \, k \leqslant g\}$ (floor function) is injected in the sampling pipeline. Consequently, an arbitrary high-dynamic-range (HDR) signal is folded back into any low-dynamic-range (LDR) ADC with range $[-\lambda, \lambda]$. This fundamentally prevents saturation or clipping. A hardware example based on modulo ADC [12] is shown in Fig. 1. The key to the HDR recovery in the USF is algorithmic "inversion" of the modulo non-linearity that amounts to "unfolding" the modulo or folded samples [12, 16, 17]. This essentially shares the same "unfolding" flavor as frequency estimation via sub-Nyquist sampling, but the subtlety here is the distinction that arises between abscissa and ordinate [18].

Motivation and Contributions. Currently, frequency estimation in the USF leverages oversampling or temporal redundancy [19]. This naturally leads one to ask the question: Can we perform *sub-Nyquist frequency estimation* or sNyq-Ψ with modulo samples? A positive answer entails several benefits because in the USF, one can

1. significantly reduce the sampling cost as modulo ADCs inherently work with low voltage ranges and consume low power [14],
2. prevent saturation or clipping resulting from arbitrary HDR input signals [12], and,
3. provide higher digital resolution for a given bit-budget Radar [15].

The key contributions of this work are as follows:

C_1) We design a novel acquisition pipeline (see Fig. 2) that achieves sNyq-Ψ given modulo folded samples leading to sub-Nyquist USF based Frequency Estimation or sNyqλ-Ψ.

C_2) We design a novel algorithm (see Algorithm 1). Unlike previous works for bandlimited signals, we show that our recovery is guaranteed independent of the sampling rate.

C_3) Taking a step closer to practice, we build custom-designed hardware to validate our approach, demonstrating its potential benefits for real-world applications (see Section 6).

2. PROBLEM FORMULATION

Let $g(t)$ denote the sinusoidal input signal

$$g(t) = \sum\nolimits_{k=0}^{K-1} c_k e^{\jmath 2\pi f_k t} \tag{2}$$

where c_k, f_k are the unknown amplitude and frequency, respectively. Without loss of generality, we assume a real-valued $g(t)$ that accurately describes the practice. By design, in USF, the modulo non-linearity is applied in the analog domain, which folds the input $g(t)$ into a LDR $[-\lambda, \lambda]$ (see Fig. 1). Thereon, the *folded signal* $\mathscr{M}_\lambda(g(t))$ is sampled in a pointwise fashion, resulting in modulo samples,

$$y_\lambda[n] = \mathscr{M}_\lambda\big(g(nT)\big) = \mathscr{M}_\lambda\left(\sum_{k=0}^{K-1} c_k e^{\jmath 2\pi \frac{f_k}{f_s} n}\right) \tag{3}$$

where $n = 0, \cdots, N-1$ and $f_s = 1/T$ is the sampling frequency. In our context, $f_s \ll 2f_{\mathsf{max}}$ where $f_{\mathsf{max}} = \max|f_k|$.

We introduce a multi-channel sampling architecture which will be elaborated in Sec. 3. This yields multiple sequences of modulo samples with distinct thresholds $\lambda_i, i = 1, 2$, as shown in Fig. 2,

$$\begin{cases} y_{\lambda_i}[n] = \mathscr{M}_{\lambda_i}\big(g(nT)\big), & i = 1, 2 \\ y'_{\lambda_i}[n] = \mathscr{M}_{\lambda_i}\big(g(nT + T_d)\big), & i = 1, 2 \end{cases}$$

where T_d is the time delay. Given the modulo samples $y_{\lambda_i}[n], y'_{\lambda_i}[n], i = 1, 2$, our goal is to design a recovery method that can retrieve the signal parameters $\{c_k, f_k\}_{k=0}^{K-1}$ with a theoretical guarantee.

3. SUB-NYQUIST USF FOR FREQUENCY ESTIMATION

As the sinusoidal signal $g(t)$ is sampled below the Nyquist rate, most recovery approaches designed for unlimited sampling, e.g. Fourier domain partitioning [12], high-order difference [11] and iterative signal sieving [17], cannot be applied in our context.

Modular Decomposition. We start with the modular decomposition property [12] which allows us to write,

$$g = \mathscr{M}_\lambda(g) + \varepsilon^g, \quad \varepsilon^g(t) = \sum\nolimits_{l=0}^{L-1} c_l \mathbb{1}_{\mathcal{D}_l}(t)$$

where $c_l \in 2\lambda\mathbb{Z}$, $\varepsilon^g(t)$ is the residue function and $\mathbb{1}_{\mathcal{D}}$ is the indicator function on domain D with $\cup_l \mathcal{D}_l = \mathbb{R}$. Let $g[n] = g(nT)$ and T is the sampling step. Denoting by $\underline{y}$ the finite difference of y, we have

$$\underline{y}[n] = \underline{g}[n] - \underline{\varepsilon}_\lambda^g[n] = \underline{g}[n] - \sum\nolimits_{l=0}^{L-1} c_l \delta[n - n_l] \tag{4}$$

where $\{n_l\}_{l=0}^{L-1}$ are the unknown folding instants—the locations where the modulo non-linearity kicks-in. The triggering rate of n_l depends on the $\mathscr{M}_\lambda$–ADC threshold λ. For a certain dynamic range, the smaller the λ, the higher the folding rate, and the larger is the number of spikes in (4). Obviously, $\underline{g}[n]$ is not necessarily bandlimited due to the frequency aliasing (or folding). In order to decouple the dual-folding between amplitude and frequency, we adopt the same strategy as in [20]; i.e., we trade the channel redundancy for oversampling, which is characterized by the following lemma:

Lemma 1. *Assume an arbitrary input signal $g(t)$ sampled by two $\mathscr{M}_\lambda$–ADCs with thresholds λ_1 and λ_2, yielding folded samples $y_{\lambda_1}[n], y_{\lambda_2}[n]$. Then, $g[n]$ can be recovered if λ_1/λ_2 is irrational.*

Proof. From (4), we have

$$\underline{y}_{\lambda_1}[n] = \underline{g}[n] - \underline{\varepsilon}_{\lambda_1}^g[n], \ \underline{y}_{\lambda_2}[n] = \underline{g}[n] - \underline{\varepsilon}_{\lambda_2}^g[n]$$

where $\underline{\varepsilon}_{\lambda_i}^g[n] = \sum_{l_i=0}^{L_i-1} c_{l_i}\delta[n - n_{l_i}], i = 1, 2$ is the residue. Computing the difference between $\underline{y}_{\lambda_1}[n]$ and $\underline{y}_{\lambda_2}[n]$ results in

$$\underline{r}_{\lambda_{1,2}} = \underline{\varepsilon}_{\lambda_2}^g[n] - \underline{\varepsilon}_{\lambda_1}^g[n] = \sum\nolimits_{l=0}^{L_1+L_2-1} c_l \delta[n - n_l] \tag{5}$$

where $c_l = 2\lambda_2 p_l - 2\lambda_1 q_l, \{p_l, q_l\} \in \mathbb{Z}^2$. Provided that λ_1/λ_2 is irrational, the integers $\{p_l, q_l\}$ can be uniquely determined from c_l,

$$2\lambda_2(p_l - p_l') = 2\lambda_1(q_l - q_l') \iff p_l = p_l', q_l = q_l' \tag{6}$$

Once $\{p_l, q_l\}$ is known, the residues $\underline{\varepsilon}^g_{\lambda_i}[n], i=1,2$ can be recovered immediately, as well as $\underline{g}[n]$. This completes the proof. □

We refer the interested readers to [20] for the proof. Lemma. 1 reveals that the one extra channel with a co-irrational threshold makes it possible to recover the HDR samples $g[n]$ at arbitrary sampling frequency f_s. However, aliasing creates ambiguity in frequency estimation. In order to eliminate this indeterminacy, applying the same channel-redundancy strategy, we have the following result:

Lemma 2. *Assume a sinusoidal signal $g(t)$ sampled by two sub-Nyquist samplers with delay T_d, which results in*

$$g_1[n] = g(nT) \text{ and } g_2[n] = g(nT + T_d). \tag{7}$$

Then, the parameters $\{c_k, f_k\}_{k=0}^{K-1}$ can be retrieved if $T_d \leq \frac{1}{2f_{\max}}$.

Proof. Let $f'_k = f_k - \lfloor f_k/f_s \rfloor f_s$ denote the aliased frequency of f_k. From the definition of (2), we have

$$\begin{cases} g_1[n] = \sum_{k=0}^{K-1} c_k e^{\jmath 2\pi \frac{f_k}{f_s} n} \\ g_2[n] = \sum_{k=0}^{K-1} c_k e^{\jmath 2\pi f_k (T_d)} e^{\jmath 2\pi \frac{f_k}{f_s} n} \end{cases} \tag{8}$$

Since $f_s \ll 2f_{\max}$, equivalently, we can rewrite (8) as

$$\begin{cases} g_1[n] = \sum_{k=0}^{K-1} c_k e^{\jmath 2\pi \frac{f'_k}{f_s} n} \\ g_2[n] = \sum_{k=0}^{K-1} c_k e^{\jmath 2\pi f_k T_d} e^{\jmath 2\pi \frac{f'_k}{f_s} n} \end{cases}$$

Since $g_i[n], i=1,2$ share the same sinusoidal components, they can be retrieved by utilizing Prony's method; let $h[n]$ with $n = 0, \cdots, K$ be the filter z-transform $\hat{h}(z) = \sum_{n=0}^{K} h[n] z^{-n} = \prod_{k=0}^{K-1}(1 - u_k z^{-1})$ where $u_k = e^{\jmath 2\pi f'_k/f_s}$, that is, its roots correspond to the frequencies u_k to be found. Then, it follows that $h[n]$ annihilates the sinusoidal sequence $g_i[n], i=1,2$:

$$\begin{aligned} (h * g_1)[n] &= \sum_{m=0}^{K} h[m] g_1[n-m] \\ &= \sum_{k=0}^{K-1} c_k u_k^n \sum_{m=0}^{K} h[m] u_k^{-m} = 0. \end{aligned} \tag{9}$$

The same applies to $g_2(n)$. Let $\mathbf{T}(\mathbf{g_1})$ denote the Toeplitz matrix constructed by $g_1[n]$. We can rewrite (9) in matrix form as $\mathbf{T}(\mathbf{g_1})\mathbf{h} = \mathbf{0}$ where $\mathbf{T}(\mathbf{g_1})$ is a rank-deficient matrix. The filter coefficients $h[n]$ can be found by solving the above linear system of equations. Thereafter, u_k can be retrieved by computing the zeros of polynomial $\hat{h}(z)$ and amplitude c_k can be found via least-squares. As soon as $\{f'_k, c_k\}_{k=0}^{K-1}$ are retrieved, the phase term $e^{\jmath 2\pi f_k T_d}$ can thereby be estimated again via least-squares. Hence, f_k can be uniquely determined from the phase term due to the constraint $T_d \leq \frac{1}{2f_{\max}}$, as well as the recovery of c_k. □

The problem can be solved when there are at least as many equations as unknowns, implying that $N \geq 2K+1$. Notice that, $\underline{g}[n]$ is still a finite sum of sinusoids

$$\underline{g}[n] = \sum_{k=0}^{K-1} c_k (e^{\jmath 2\pi \frac{f_k}{f_s}} - 1) e^{\jmath 2\pi \frac{f_k}{f_s} n}$$

which allows for parameter retrieval in the finite difference domain. Combining the ingredients above, we finally have the following result on sub-Nyquist unlimited sampling:

Algorithm 1 `sNyq`λ-Ψ: Frequency Retrieval via Sub-Nyquist USF

Input: Modulo Samples $y_{\lambda_i}[n], y'_{\lambda_i}[n], i=1,2$.
  Compute the residue difference $\underline{r}_{\lambda_{1,2}}$ via (5).
  for $i = 0$ to $L_1 + L_2 - 1$ **do**
    Find the integers $\{p_l, q_l\}$ via (6).
  end for
  Recover $\underline{g}(nT)$ via (4).
  Recover $\underline{g}(nT + T_d)$ from $y'_{\lambda_i}[n], i=1,2$.
  Estimate $\{f'_k\}_{k=0}^{K-1}$ via (9).
  Determine $\{f_k\}_{k=0}^{K-1}$ from the fitted phase.
Output: Signal parameters $\{f_k, c_k\}_{k=0}^{K-1}$.

Theorem 1. *Assume a sinusoidal signal $g(t)$ sampled by a four-channel sampling architecture as described in Fig. 2. Then, the signal parameters $\{c_k, f_k\}_{k=0}^{K-1}$ can be perfectly retrieved if λ_1/λ_2 is irrational and $T_d \leq \frac{1}{2f_{\max}}$.*

Theorem 1 shows that leveraging inter-channel redundancy enables HDR `sNyq`λ-Ψ, which significantly reduces the sampling cost and power consumption (see hardware experiments in Sec. 6). More concretely, by utilizing additional sampling channels with distinct thresholds and time delays, we are able to decouple amplitude-frequency folding and retrieve the signal parameters. An efficient implementation of our recovery method is outlined in Sec. 4.

4. RECOVERY ALGORITHM

Let $y_{\lambda_i}[n] = \mathscr{M}_{\lambda_i}(g(nT)), y'_{\lambda_i}[n] = \mathscr{M}_{\lambda_i}(g(nT+T_d)), i=1,2$ denote the measurements. Below, we outline the steps of our recovery method.

Step 1: Amplitude Unfolding. We compute the difference $\underline{r}_{\lambda_{1,2}} = \underline{y}_{\lambda_1} - \underline{y}_{\lambda_2}$. From Lemma 1, we have $\underline{r}_{\lambda_{1,2}} = \underline{\varepsilon}^g_{\lambda_2}[n] - \underline{\varepsilon}^g_{\lambda_1}[n]$, from which the integer folding times can be retrieved via (6). Thereon, $\underline{\varepsilon}^g_{\lambda_1}[n], \underline{\varepsilon}^g_{\lambda_2}[n]$ can be exactly recovered. Then, $\underline{g}[n]$ can be reconstructed using (4) (the same steps apply for $y'_{\lambda_i}, i=1,2$).

Step 2: Frequency Unfolding. From retrieved $\underline{g}(nT)$, we can estimate the folded frequencies f'_k via (9) and amplitudes through least-squares. Given retrieved $\{f'_k, c_k\}_{k=0}^{K-1}$ and $\underline{g}(nT+T_d)$, we determine $\{f_k, c_k\}_{k=0}^{K-1}$ from the fitted phase via least-squares.

Fig. 2 describes the signal reconstruction process. An algorithmic implementation is provided in Algorithm. 1.

5. NUMERICAL EXPERIMENTS

We conduct numerical experiments to validate the proposed sampling scheme. We use the mean-squared error between f_k and $\widetilde{f}_k$

$$\text{MSE}(f_k, \widetilde{f}_k) = \frac{1}{K} \sum_{k=0}^{K-1} \left| f_k - \widetilde{f}_k \right|^2$$

to evaluate the accuracy of frequency estimation. The experimental settings and results are tabulated in Table. 1. In all scenarios, we achieve frequency estimation up to machine precision.

6. HARDWARE EXPERIMENTS

To assess the practicability and robustness of our method, we perform hardware experiments based on $\mathscr{M}_\lambda$–`ADC` that implements the proposed sampling pipeline described in Fig. 2.

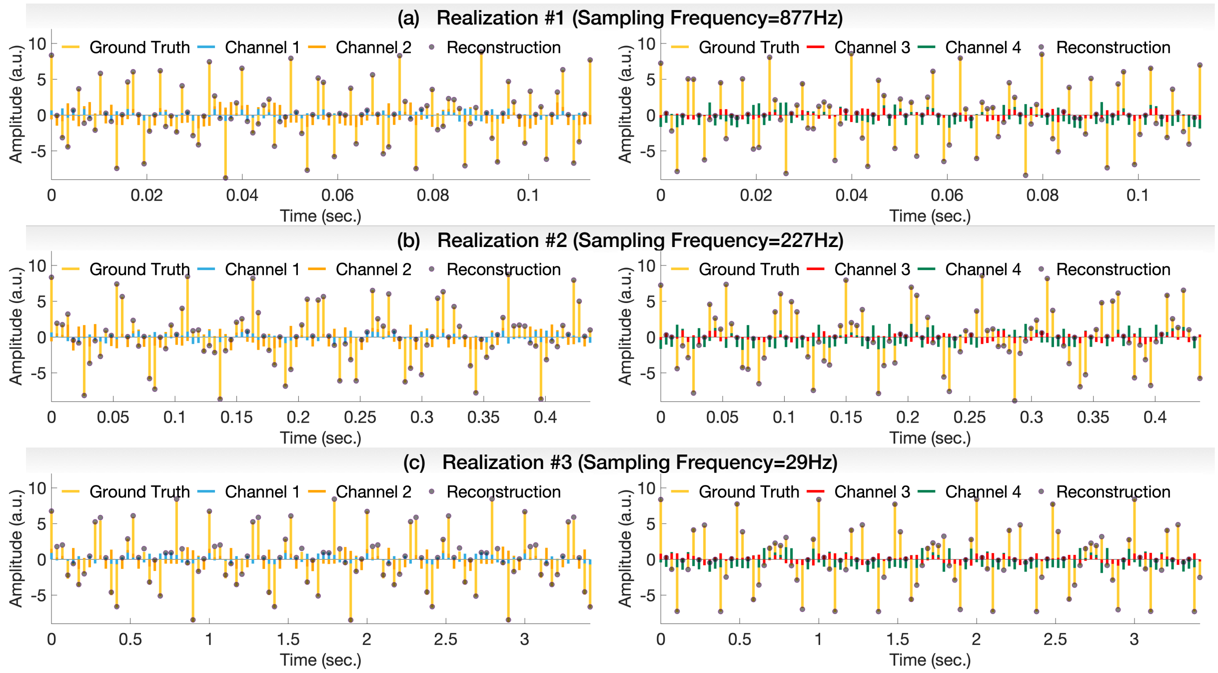

Fig. 3: Hardware Experiment: Recovery from sub-Nyquist modulo samples. The frequencies to be estimated are $f_k = [400, 700, 1000]$ Hz. We conduct 3 experiments with different sampling rates: (a) 877 Hz, (b) 227 Hz and (c) 29 Hz. In all realizations, the estimation is very accurate with $\mathrm{MSE}(f_k, \widetilde{f}_k) < 4\times 10^{-6}$.

Table 1: Summary of Experimental Parameters and Performance Evaluation.

Exp. No.	N	f_s	T_d	λ_1	λ_2	$\|g\|_\infty$	f_k	$\mathrm{MSE}(f_k, \widetilde{f}_k)$
		(Hz)	(μs)				(Hz)	
I	29	1	1	0.14	0.1	8.39	[106.9,195.1,134.5,103.6]	5.05×10^{-29}
I	29	1×10^{-2}	1	0.14	0.1	8.39	[106.9,195.1,134.5,103.6]	2.52×10^{-28}
I	29	1×10^{-3}	1	0.14	0.1	8.39	[106.9,195.1,134.5,103.6]	2.52×10^{-28}

Experimental Protocol. The HDR input signal is generated by TG-5011A signal generators via amplitude modulation (AM). For each experiment, we simultaneously acquire modulo samples from the multi-channel $\mathscr{M}_\lambda$–`ADC` devices with tunable thresholds. We simultaneously plot the input and output of the multi-channel $\mathscr{M}_\lambda$–`ADC` on the `PicoScope 3406D` oscilloscope to obtain the ground-truth. A 6-bit sampler is used to sample the analog waveforms. Given the 6-bit resolution, the samples are effectively quantized by a 6-bit, uniform quantizer and thus, the signal measurements are inevitably contaminated by quantization noise. We fix the input HDR signal and decrease the sub-Nyquist sampling frequency from 877 Hz to 29 Hz. For each experiment, we report the numerical values for,

—• the sampling frequency f_s and delay T_d.
—• the sampling thresholds $\lambda_i, i = 1, 2$.
—• the dynamic range of the input signal $\|g\|_\infty = \max |g|$.
—• the number of samples N.
—• the MSE of frequency estimation.

The experimental parameters and results are summarized in Table 2.

Table 2: Summary of Experimental Parameters and Performance Evaluation.

Figure	N	f_s	T_d	λ_1	λ_2	$\|g\|_\infty$	f_k	$\widetilde{f}_k$	$\mathrm{MSE}(f_k, \widetilde{f}_k)$
		(Hz)	(ms)	(V)	(V)	(V)	(Hz)	(Hz)	
Fig. 3 (a)	200	877	0.2	1.0	1.9	8.88	[400, 700, 1000]	[400, 700, 1000]	2.14×10^{-6}
Fig. 3 (b)	200	227	0.2	1.0	1.9	8.92	[400, 700, 1000]	[400, 700, 1000]	3.09×10^{-6}
Fig. 3 (c)	100	29	0.2	1.0	1.9	8.82	[400, 700, 1000]	[400, 700, 1000]	4.33×10^{-7}

We plot the amplitude-unfolding of the HDR input signal under different sub-Nyquist sampling frequencies in Fig. 3. For each experiment, the signal has a large dynamic range: $\|g\|_\infty = 9.18\lambda_1 = 4.79\lambda_2$. The co-irrational threshold design makes it possible to sample sinusoidal signals with large amplitudes, which fundamentally eliminates the bottlenecks of dynamic range and digital resolution in the conventional Shannon-Nyquist sensing pipeline. As $f_{\mathsf{max}} = 1000$ Hz, the standard Nyquist sampling frequency is 2000 Hz. Thanks to the proposed sampling pipeline, we are able to achieve accurate frequency estimation with 43.9%, 13.9% and 1.45% of the Nyquist frequency, which significantly reduces the sampling cost. As shown in Fig. 3, despite the bit budget of the sampler, the HDR signals are accurately reconstructed in all realizations, yielding accurate frequency retrievals as tabulated in Table. 2. These hardware experiments effectively demonstrate the high practical utility and robust performance of the proposed sampling scheme in a variety of applications.

7. CONCLUSION

In this paper, we have proposed a novel method for frequency estimation from sub-Nyquist, modulo samples. Our approach is based on a co-design strategy. On the hardware front, we have developed a multi-channel architecture that enables sub-Nyquist folded sampling. On the algorithms front, our algorithm performs HDR unfolding. Thanks to the customized sensing pipeline, different from previous approaches, our sampling guarantee is independent of input bandwidth. Due to the co-design approach, our work opens up new capabilities for the field. Our algorithmic machinery directly enables sub-Nyquist applications such as radar sensing [15] and DOA estimation [21] in the USF context. Furthermore, our work prompts towards new directions including, a) bandwidth-extension or extending the bandwidth of modulo ADCs designed for lower sampling rates, b) efficient design of multi-channel hardware, c) investigation of new architectures that can further minimize the number of channels.

8. REFERENCES

[1] X.-G. Xia, "On estimation of multiple frequencies in undersampled complex valued waveforms," *IEEE Trans. Sig. Proc.*, vol. 47, no. 12, pp. 3417–3419, Dec. 1999.

[2] G. Zhou and X.-G. Xia, "Multiple frequency detection in undersampled complex-valued waveforms with close multiple frequencies," *Electronics Letters*, vol. 33, no. 15, p. 1294, Jul. 1997.

[3] L. Xiao and X.-G. Xia, "A generalized Chinese remainder theorem for two integers," *IEEE Signal Process. Lett.*, vol. 21, no. 1, pp. 55–59, Jan. 2014.

[4] W. Wang, X. Li, W. Wang, and X.-G. Xia, "Maximum likelihood estimation based robust Chinese remainder theorem for real numbers and its fast algorithm," *IEEE Trans. Sig. Proc.*, vol. 63, no. 13, pp. 3317–3331, Jul. 2015.

[5] L. Xiao and X.-G. Xia, "Frequency determination from truly sub-Nyquist samplers based on robust Chinese remainder theorem," *Signal Processing*, vol. 150, pp. 248–258, Sep. 2018.

[6] N. Fu, G. Huang, L. Zheng, and X. Wang, "Sub-Nyquist sampling of multiple sinusoids," *IEEE Signal Process. Lett.*, vol. 25, no. 4, pp. 581–585, Apr. 2018.

[7] P. P. Vaidyanathan and P. Pal, "Sparse sensing with co-prime samplers and arrays," *IEEE Trans. Sig. Proc.*, vol. 59, no. 2, pp. 573–586, Feb. 2011.

[8] A. Bhandari and R. Raskar, "Signal processing for time-of-flight imaging sensors: An introduction to inverse problems in computational 3-D imaging," *IEEE Signal Process. Mag.*, vol. 33, no. 5, pp. 45–58, Sep. 2016.

[9] S. Qin, Y. D. Zhang, M. G. Amin, and A. M. Zoubir, "Generalized coprime sampling of toeplitz matrices for spectrum estimation," *IEEE Trans. Sig. Proc.*, vol. 65, no. 1, pp. 81–94, Jan. 2017.

[10] A. Bhandari, F. Krahmer, and R. Raskar, "On unlimited sampling," in *Proc. Int. Conf. Sampling Theory Appl.* IEEE, Jul. 2017.

[11] ——, "On unlimited sampling and reconstruction," *IEEE Trans. Sig. Proc.*, vol. 69, pp. 3827–3839, Dec. 2021.

[12] A. Bhandari, F. Krahmer, and T. Poskitt, "Unlimited sampling from theory to practice: Fourier-Prony recovery and prototype ADC," *IEEE Trans. Sig. Proc.*, vol. 70, pp. 1131–1141, Sep. 2022.

[13] A. Bhandari, "Back in the US-SR: Unlimited sampling and sparse super-resolution with its hardware validation," *IEEE Signal Process. Lett.*, vol. 29, pp. 1047–1051, Mar. 2022.

[14] Z. Liu, A. Bhandari, and B. Clerckx, "λ–MIMO: Massive MIMO via modulo sampling," *IEEE Trans. Commun.*, vol. 71, no. 11, pp. 6301–6315, Nov. 2023.

[15] T. Feuillen, B. S. MRR, and A. Bhandari, "Unlimited sampling radar: Life below the quantization noise," in *IEEE Intl. Conf. on Acoustics Speech and Sig. Proc. (ICASSP)*. IEEE, Jun. 2023.

[16] D. Florescu, F. Krahmer, and A. Bhandari, "The surprising benefits of hysteresis in unlimited sampling: Theory, algorithms and experiments," *IEEE Trans. Sig. Proc.*, vol. 70, pp. 616–630, Jan. 2022.

[17] R. Guo and A. Bhandari, "ITER-SIS: Robust unlimited sampling via iterative signal sieving," in *IEEE Intl. Conf. on Acoustics Speech and Sig. Proc. (ICASSP)*. IEEE, Jun. 2023.

[18] Y. Gong, L. Gan, and H. Liu, "Multi-channel modulo samplers constructed from Gaussian integers," *IEEE Signal Process. Lett.*, vol. 28, pp. 1828–1832, 2021.

[19] A. Bhandari, F. Krahmer, and R. Raskar, "Unlimited sampling of sparse sinusoidal mixtures," in *IEEE Int. Symp. Inf.* IEEE, Jun. 2018.

[20] R. Guo and A. Bhandari, "Unlimited sampling of FRI signals independent of sampling rate," in *IEEE Intl. Conf. on Acoustics Speech and Sig. Proc. (ICASSP)*. IEEE, Jun. 2023.

[21] S. Fernandez-Menduina, F. Krahmer, G. Leus, and A. Bhandari, "Computational array signal processing via modulo non-linearities," *IEEE Trans. Sig. Proc.*, vol. 70, pp. 2168–2179, Mar. 2022.